Special issue article

SURFACE and INTERFACE ANALYSIS

Received: 31 March 2017 Revised: 23 August 2017 Accepted: 23 August 2017 Published online in Wiley Online Library: 29 September 2017

(wileyonlinelibrary.com) DOI 10.1002/sia.6315

Time-of-flight secondary ion mass spectrometry analysis of paint craters

Heather L. Bloomfield[a]* and Heng-Yong Nie[a,b]

Localized sudden changes in the surface energy of a surface to be painted are commonly held responsible for causing paint craters. However, it is not necessarily an easy task to identify the material(s) that produced the defects. Automotive paint cratering, when it happens, often requires immediate identification of its causes because the product line may have to be shut down until the problem is solved. For the past 18 years, Surface Science Western has applied time-of-flight secondary ion mass spectrometry (ToF-SIMS), among other techniques, to help its clients in the automotive industry identify the chemicals responsible for producing paint craters. In this article, we demonstrate that ToF-SIMS is a unique and powerful technique in identifying the chemicals such as siloxane, fluorocarbons and fatty acids that are responsible for causing paint craters. We further show that the chemicals can be foreign contaminants, as well as segregation of additives in the paint systems, and even from contaminated solvents used in the paint. When the chemicals causing the paint craters can be identified by ToF-SIMS analysis, the automotive company can often track down the primary source and remove the root cause. As such, surface analysis and in particular ToF-SIMS is invaluable in understanding paint cratering for both the surface analysis research community and paint manufacturers and users. Copyright © 2017 John Wiley & Sons, Ltd.

Keywords: ToF-SIMS; paint craters; surfactants; siloxane; fluorocarbon

Introduction

Automotive painting amounts to a major portion of the production cost for a vehicle because of the energy consumed in the painting process.[1] It is thus important to make sure the finished paint wets the surface completely and is defect free. The two most critical parameters to ensure a smooth and defect-free paint film[2] are the surface energy γ_S of the surface to be painted and the surface tension γ_L of the paint.[3] When a liquid droplet is placed on a solid surface, it will either bead up partially or completely wet the substrate, depending on the surface tensions of the liquid and the solid. Figure 1 shows a liquid droplet on a substrate, in its equilibrium state, with a contact angle θ. Also shown in the figure is the liquid–vapour surface tension γ_{LV}, the solid–vapour surface tension γ_{SV} and the solid–liquid interfacial tension γ_{SL}. When these forces at the contact line balance, the liquid droplet will reach its equilibrium state, which is expressed by Young's equation $\gamma_{SV} - \gamma_{SL} - \gamma_{LV}\cos\theta = 0$. It is obvious that when $\theta = 0$, the liquid droplet completely wets the solid surface. A general rule for a liquid to wet the substrate it is placed on is that the spreading coefficient,[4] $S = W_a - W_c$, must be positive, where W_a is the work of adhesion and W_c work of cohesion.[5–9] The spreading coefficient can be intuitively understood in that the liquid will completely wet the surface if its attraction with the substrate is stronger than its attraction with itself.

With $W_a = \gamma_{SV} + \gamma_{LV} - \gamma_{SL}$ and $W_c = 2\gamma_{LV}$, one arrives at $S = \gamma_{SV} - (\gamma_{SL} + \gamma_{LV})$. Although the dynamics[5] of the wetting of a liquid on a solid surface is more complicated,[6–8] Young's equation and spreading coefficient are adequate for us to qualitatively understand the wetting of paint on a substrate. If the surface energy of the surface to be painted is fixed, then the surface tension of the paint should be as small as possible for the paint to wet the surface. Therefore, for a paint to work well with a surface, a paint formulation requires the use of surfactants to reduce the surface tension of the paint.[1,9,10] Paint formulators typically incorporate either hydrocarbon, siloxane or fluorocarbon surfactants into their paint formulations. This is especially true for water base systems, because of the rather large surface tension of water (72 mN/m). Among the three types of surfactants, fluorocarbon surfactants have the smallest surface tensions, usually less than 20 mN/m, followed by siloxane and hydrocarbon surfactants having a surface tension of ~24 and <30 mN/m, respectively.[11,12]

Paint craters often happen when there is a contaminant present on the surface that has a surface energy less than the surface tension of the paint to be applied. As shown in Fig. 2, because of their low surface energies, the presence of these materials on the substrate will likely cause paint cratering[13] as the paint will dewet. It is worth noting that even if the surface energy of the particle shown in the figure is not especially low, a defect may still form because of the incompatibility between the particle and the paint.

Figure 3a–c shows the optical, scanning electron microscope and profilometry images, respectively, obtained on a paint crater. Figure 3d shows that the crater is 45 μm deep. Not only is the crater visually distinctive within an automobile paint layer but the thinning of the paint will also diminish the protection of the paint. It is therefore imperative that the cause of the crater be identified.

* *Correspondence to: H. L. Bloomfield, Surface Science Western, The University of Western Ontario, 999 Collip Circle, London N6G 0J3 Ontario, Canada. E-mail: hbloomf@uwo.ca*

a *Surface Science Western, The University of Western Ontario, London N6G 0J3, Ontario, Canada*

b *Department of Physics and Astronomy, The University of Western Ontario, London N6A 3K7, Ontario, Canada*

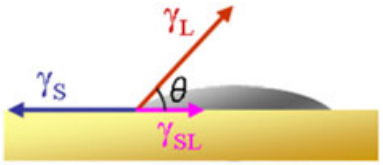

Figure 1. Young's observation on contact angle formed by a liquid droplet placed on a solid surface. The equilibrium contact angle (θ) is such that the lateral force at the point where air, liquid and solid meet be kept balanced. The three forces are the solid–vapour interface tension (γ_{SV}), liquid–vapour interface tension (γ_{LV}) and solid–liquid interface tension (γ_{SL}).

Figure 2. Illustration of paint crater formation caused by a contaminant with low surface energy, from which the applied paint is displaced.

As even a monolayer of contamination can cause such defects, surface sensitive analytical techniques are required. While complimentary techniques are available, time-of-flight secondary ion mass spectrometry (ToF-SIMS) has certain advantages[14,15] over other techniques, thereby making it the technique of choice in many instances. While ToF-SIMS has been used to find industrial solutions,[16,17] little has been reported on when it comes to paint crater analysis.[18–21]

In ToF-SIMS, a pulsed primary ion beam is used to bombard the sample surface to generate particles that are mostly neutrals with electrons and ions. These secondary ions, with a kinetic energy determined by the extraction voltage and the charge it carries, traverse the flight tube and arrive at the detector according to their times of flight, which are a function of their mass. The arrival time of an ion is converted to its mass to charge ratio (m/z). A secondary ion mass spectrum is the intensities of ions against their m/z. The detection limit of ToF-SIMS is believed to be in the range of 1 ppb to 1 ppm, depending on element or ion species. However, ToF-SIMS is not a quantitative technique because ion yields are significantly different for different elements and molecules. These different ion yields may vary significantly according to chemical environments (matrix effect).

Because the information ToF-SIMS provides are the mass of chemicals or their fragments, it provides unique specificity. The molecular ion, either the molecule itself, protonated or deprotonated is detected for many materials. For example, for the two most encountered fatty acids palmitate and stearate, whose masses are m/z 28 (C_2H_4) apart, ToF-SIMS provides direct identification for their molecular ions $C_{16}H_{31}O_2^-$ and $C_{18}H_{35}O_2^-$ at m/z 255 and 283, respectively. Other examples of materials we have examined include deprotonated erucamide ion $C_{22}H_{42}NO^-$ (m/z 336), dodecyl sulfate $C_{12}H_{25}SO_4^-$ (265), dodecylbenzenesulfonate $C_{18}H_{29}SO_3^-$ (325), octadecylphosphonate[22] $C_{18}H_{38}PO_3^-$ (334) and dimethyldioctadecylammonium ion[23] $C_{38}H_{80}N^+$ (551). For the two most common cratering agents siloxanes and fluorocarbons,[1] they have diagnostic ions, both negative and positive, which allows ToF-SIMS to easily identify these two chemicals. Their ion fragmentation patterns will be discussed later in detail.

ToF-SIMS is also a valuable technique because of its imaging capabilities with relatively high spatial resolution (~2 μm) in the high mass resolution mode.[24] For instance, if a crater contains a localized contaminant at the centre, the contaminant may not be readily determined solely from the secondary ion mass spectra but is visible when ion imaging is used.

Other techniques that are often used in crater analysis, especially if ToF-SIMS is unavailable, are scanning electron microscopy coupled with energy dispersive X-ray spectroscopy (SEM/EDX), Fourier-transform infrared spectroscopy (FTIR) and/or X-ray photoelectron spectroscopy (XPS). Although these techniques can be valuable in determining the cause of a crater, we have found that

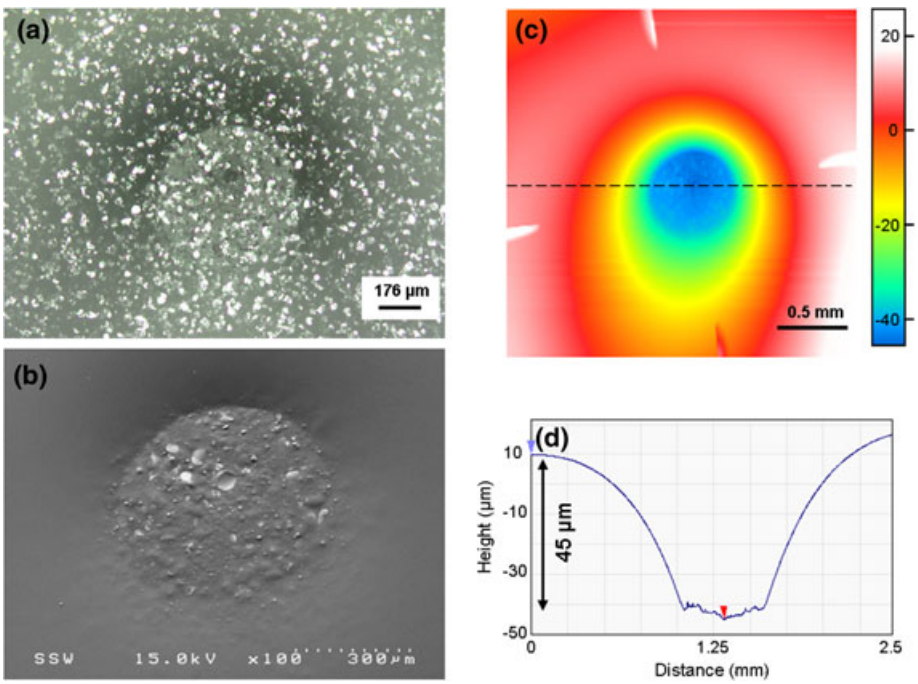

Figure 3. (a) Optical, (b) scanning electron microscope and (c) profilometry images of the same crater. The false colour height scale in μm is shown beside the surface morphology in (c). The crater is 45 μm deep as shown by the profile (d) isolated from (c) indicated by the broken line.

in most instances, ToF-SIMS is superior in its sensitivity and chemical selectivity. FTIR spectroscopy provides compositional information, but it does not have the same surface sensitivity as ToF-SIMS, and, more often than not, the crater has formed because of a contaminant that is either too small for FTIR analysis or is not visible in the crater. SEM/EDX allows for the analysis of smaller visible contaminants, but it only provides elemental, not chemical structural information. Because ToF-SIMS is only qualitative, sometimes XPS, which is quantitative, will be used in conjunction with ToF-SIMS. For example, if siloxane is detected in a crater using ToF-SIMS but the peak intensities are very similar to that of the siloxane detected away from the crater, XPS will be used to determine if there is a quantifiable difference that could account for the crater formation. However, XPS does not have the same surface sensitivity and chemical selectivity in identifying chemical structures, as well as the superior mapping capabilities that ToF-SIMS provides.

We present in this Surface Science Western special issue several typical examples from our ToF-SIMS analysis of paint craters in the hope that this will help increase the awareness of ToF-SIMS as a powerful analytical technique to provide automotive and paint companies clues towards solving their paint cratering issues.

Experimental

Samples, once received, were kept as clean as possible[21] and cut to the appropriate size prior to analysis with no further sample preparation. ToF-SIMS was performed using an ION-TOF (GmbH, Germany) ToF-SIMS IV with a bismuth liquid metal ion source. The base pressure of the analysis chamber was ~10^{-8} mbar. The 25 keV Bi_3^+ primary ion beam was pulsed at a 1 ns width, generating a target current of ~1 pA. In most cases, the Bi_3^+ beam was rastered over an area of 500 × 500 μm at 128 × 128 pixels. The action of the primary ion beam bombardment on the sample surface induces the emission of positive and negative secondary ions (as well as neutral species and electrons). These secondary ions are extracted using an extraction voltage of 2000 V from the sample surface and mass separated via a reflectron-type of ToF analyser. The ions, either positive or negative at a time, traverse the flight tube and arrive at the detector at a time according to their m/z. At each and every pixel where the primary ion beam bombarded the surface, a spectrum was obtained. An ion image was constructed by plotting the intensity of that ion against all pixels. Ion mass spectra were calibrated using hydrogen and carbon, or other known species. The mass resolution for spectra obtained in the rather large area (500 × 500 μm) was 3000–4000 for $C_3H_5^+$ and $C_4H_9^+$. The m/z range was 1–900 with a cycle time of 100 μs; higher m/z ranges were possible with longer cycle times. Because of the insulating nature of the samples, a pulsed electron flood gun was employed for charge neutralization at the end of each cycle time.

Examples of craters investigated using time-of-flight secondary ion mass spectrometry

Fluorocarbon contamination

Although siloxanes and fluorocarbons are used as additives in paint to lower the surface tension of the paint, they are also the most common cratering agents encountered because of their low surface tension. In certain instances, when a crater is caused by a fluorocarbon, there is a small particle at or near the centre of the crater, where the paint has dewetted by the low surface energy material. Because of the small size of the particle, it is often difficult to identify the contaminant using FTIR spectroscopy. Fluorine can be detected by SEM/EDX spectroscopy, but with only elemental identification, it is difficult to determine what type of material the fluorine arises from. However, as shown in Figs 4a and 4b, ToF-SIMS readily identifies a perfluorocarbon (e.g. Teflon™) and a perfluoroether (e.g. Krytox™) in individual craters, respectively.

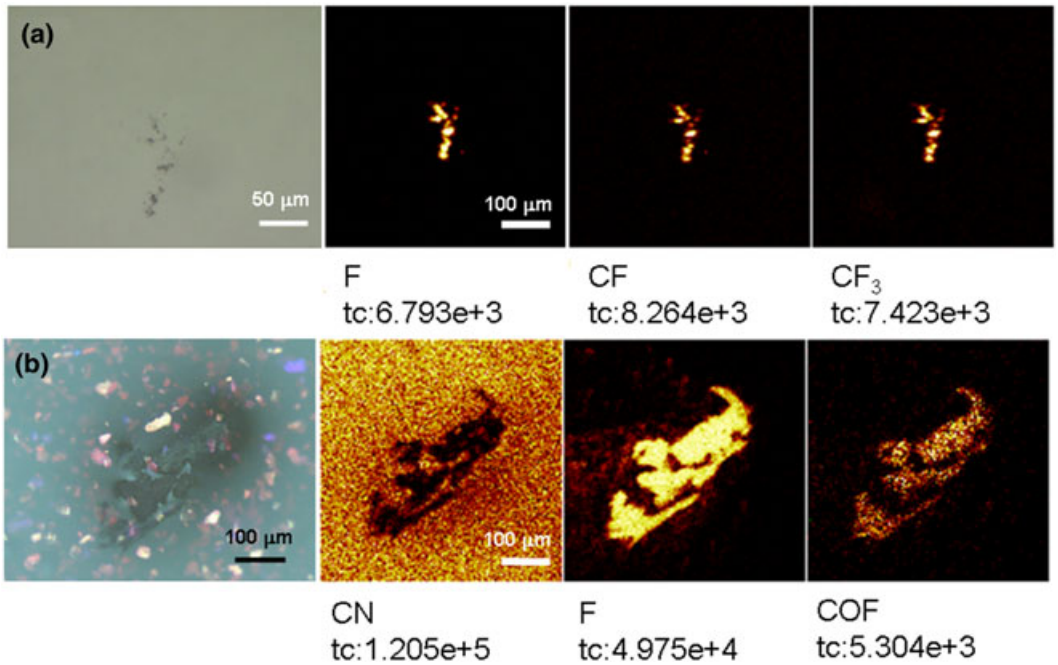

Figure 4. (a) Optical image and ion images of F^-, CF^+ and CF_3^+ for a crater containing a perfluorocarbon and (b) optical image and ion images of CN^-, F^- and COF^- for a perfluoroether.

The characteristic ion fragments for perfluorocarbons include F^- (19), C^+ (12), $CF^{+/-}$ (31), $CF_3^{+/-}$ (69), $C_3F_5^+$ (131) and other $C_xF_y^{+/-}$ species, while for perfluoroethers, they are F^-, COF_3^- (85), $C_2OF_5^-$ (135), $C_3O_2F_5^-$ (163), $C_3OF_7^-$ (185), C^+, CF^+, $COF^{+/-}$ (47), $CF_3^{+/-}$, $C_2OF_3^+$ (97), $C_3OF_5^+$ (147) and other $C_xO_yF_z^{+/-}$ species. ToF-SIMS is also useful in the identification of other fluorine-containing polymers such as polyvinylidene fluoride or polyvinyl fluoride, each of them has its own diagnostic ions. It is worth mentioning that fluorine originating from (inorganic) fluorides can be easily differentiated from fluorocarbons as there are no ions containing both fluorine and carbon. Another immediate sign of the presence of fluorocarbons is that C^+ is more abundant than CH^+.

Some uses of fluorocarbons include lubricants, pipes and fixtures such as washers and connectors. In the case that these are fractured or released, they may land on the surface to be painted or become incorporated into the paint and most likely cause a crater. In certain instances, a suspect material may be provided so that the cause of the crater is identified and removed.

A prime example of how ToF-SIMS was able to match a crater contaminant to a suspect material is presented in Fig. 5. The ToF-SIMS analysis of the crater detected fluorocarbon fragments and chlorine. A suspect glove was analysed for comparison, and the coating on the glove contained the same fragments to what was detected in the crater. Eliminating the use of the gloves from the paint site resulted in a large decrease in craters.

As shown in Fig. 6, EDX analysis of a similar crater only detected elements common to the clearcoat, and chlorine and fluorine were not detected. The EDX results thus prove that the contaminant in the crater was too thin for EDX to detect. This is a perfect example of how the surface sensitivity of ToF-SIMS was able to identify the source of the crater contamination, where other techniques are lacking.

Siloxane contamination

Siloxanes are another common cratering agent because their surface tension is as small as ~24 mN/m. Analysis of one particular crater determined that a siloxane contaminant in a paint solvent was causing craters when the paint was applied. Figure 7 shows the ToF-SIMS spectrum of the residue of a suspect paint solvent after evaporation in a clean aluminium boat. Characteristic siloxane ions $SiC_3H_9^+$ (73) and $Si_2C_5H_{15}O^+$ (147) can be seen, which are absent in the control solvent. The presence of siloxane is further confirmed by the other characteristic ions (not shown) $Si_3C_5H_{15}O_3^+$ (207), $Si_3C_7H_{21}O_2^+$ (221) and $Si_4C_7H_{21}O_4^+$ (281).

Although the detection of siloxane in a crater is usually straightforward, it can be difficult to determine what type of siloxane is causing the crater, especially when the paint contains siloxane as an additive. In certain instances, with the use of ToF-SIMS, we can narrow down what type of siloxane may be present in the crater.[18] Presented in Fig. 8a is an optical microscope image of a crater showing a contaminant with a birefringent pattern, whose location is indicated by the circle. The negative ion mass spectrum shown in the upper panel of Fig. 8b shows that the crater contains siloxane. As shown in the lower panel of Fig. 8b, the clearcoat reference (i.e. the area away from the crater) also contains siloxane. The common negative ions for siloxane are $SiC_2H_5O^-$ (73), $SiCH_3O_2^-$ (75), $SiC_3H_9O^-$ (89), $SiC_2H_7O_2^-$ (91), $Si_2C_3H_9O_3^-$ (149), $Si_2C_5H_{15}O_2^-$ (163), $Si_2C_4H_{13}O_3^-$ (165), $Si_3C_5H_{15}O_4^-$ (223) and $Si_3C_7H_{21}O_3^-$ (237).

Although siloxane was detected both in the crater and the clearcoat, the ion ratios are different. We have confirmed that the fragmentation pattern of negative siloxane ions can vary depending on the type of siloxane used. For example, the siloxane contaminant detected in the crater contains stronger negative ions at $SiC_2H_7O_2^-$ (91), $Si_2C_3H_9O_3^-$ (149) and $Si_3C_5H_{15}O_4^-$ (223), whereas the siloxane in the clearcoat has strong negative ions at $Si_2C_5H_{15}O_2^-$ (163) and $Si_3C_7H_{21}O_3^-$ (237). Based on these differences, we inferred that the siloxane concentrated in the crater is not the same as the siloxane additive in the clearcoat.

Our ToF-SIMS work dealing with numerous types of siloxanes suggests that for pure polydimethylsiloxane, the intensities of the negative ions $SiC_3H_9O^-$ (89) and $Si_2C_5H_{15}O_2^-$ (163) are larger than those $SiC_2H_7O_2^-$ (91) and $Si_2C_4H_{13}O_3^-$ (165), respectively, which has also been discussed before.[18] While for cross-linked siloxanes[25] or cyclosiloxanes, the ion intensity for these two pairs of negative ions were reversed. Our explanation is that the two peaks at m/z 89 and 163 ($SiC_3H_9O^-$ and $Si_2C_5H_{15}O_2^-$) both have a group with an Si atom bonded to three methyl (CH_3) groups, while in the two peaks at m/z 91 and 165 ($SiC_2H_7O_2^-$ and $Si_2C_4H_{13}O_3^-$), all Si atoms are bonded to only two methyl groups. The presence of

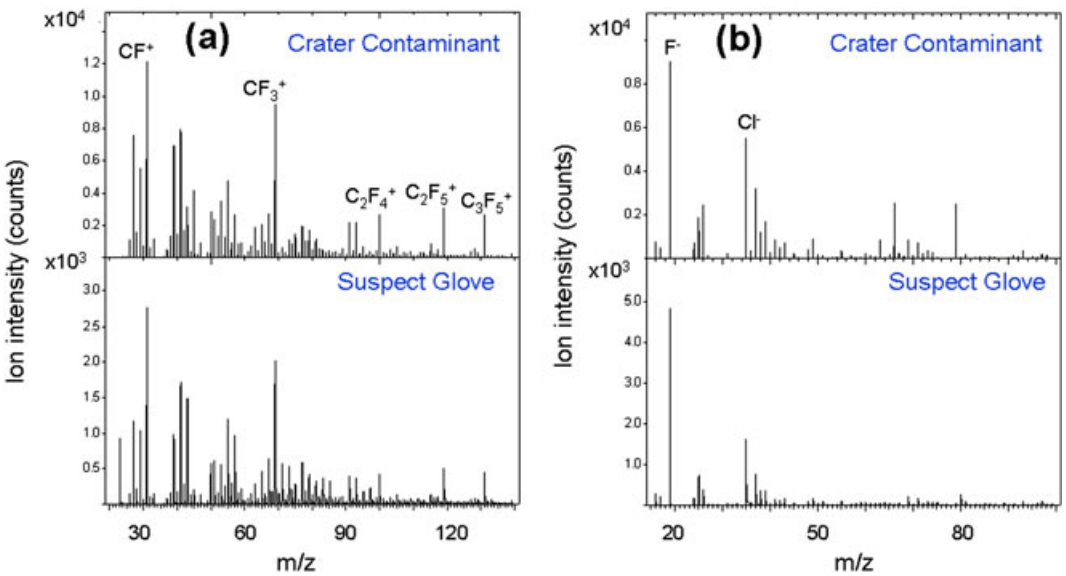

Figure 5. (a) Positive and (b) negative secondary ion mass spectra collected from a crater (upper panel) and coating on suspect glove (lower panel).

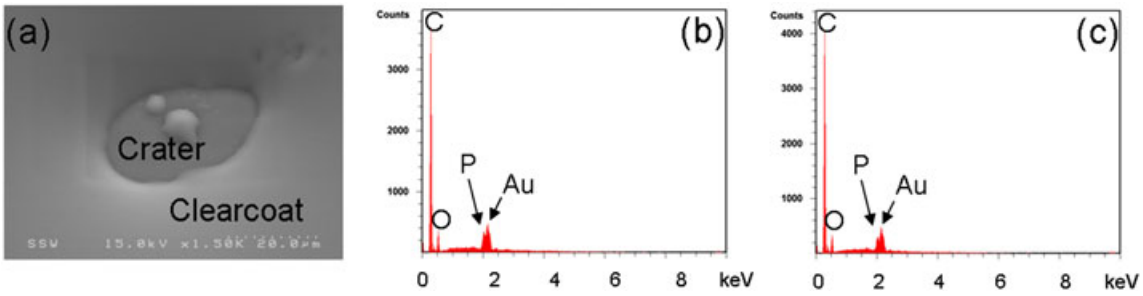

Figure 6. (a) Scanning electron microscopy image and energy dispersive X-ray spectroscopy spectra collected from the (b) crater and (c) clearcoat.

end groups of $-Si(CH_3)_3$ in a siloxane structure prefers to enhance the ion yield of $SiC_3H_9O^-$ (89) over $SiC_2H_7O_2^-$ (91) and $Si_2C_5H_{15}O_2^-$ (163) over $Si_2C_4H_{13}O_3^-$ (165). We also noticed that $-Si(CH_3)_3$ groups favour the formation of the negative ion $Si_3C_7H_{21}O_3^-$ (237). Therefore, ToF-SIMS can be used to differentiate the structures of siloxanes by comparing ion intensity ratios between $SiC_3H_9O^-$ and $SiC_2H_7O_2^-$, as well as between $Si_2C_5H_{15}O_2^-$ and $Si_2C_4H_{13}O_3^-$. These are the common cases that we have dealt with. There may be other chemical structural differences (e.g. different end groups, block copolymers and branched polymers) that can cause changes in relationships among the siloxane ions.

Aggregated additives

Paint is a rather complex system containing multiple ingredients, each brought in to meet a specific aspect of the designed paint performance or property, such as wettability, drying dynamics, mechanical strength and chemical stability. Therefore, even without a foreign contaminant, any incompatibility among the ingredients or imperfection of any ingredient may find a way to manifest as a paint defect.

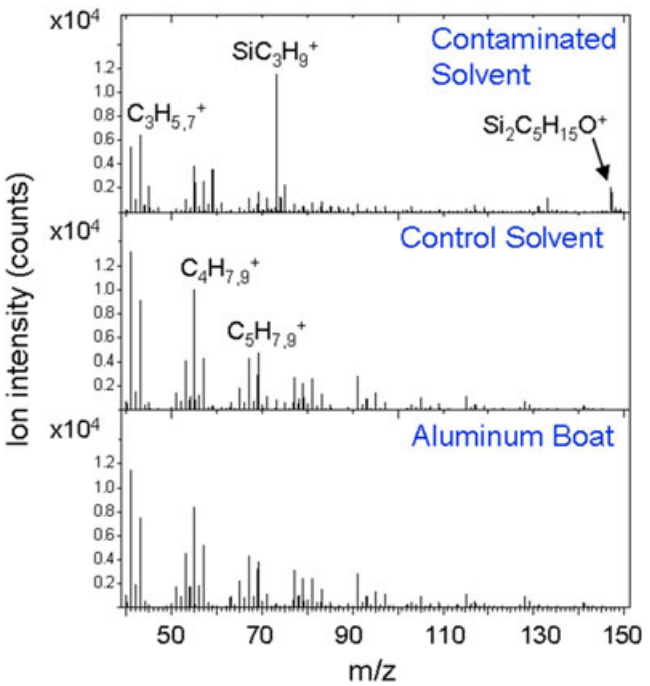

Figure 7. Positive secondary ion mass spectra collected from the residue of a contaminated solvent and a control solvent prepared on clean aluminium boats, as well as a clean aluminium boat.

Shown in Fig. 9a are an optical microscope image and images of CN^- and negative ions at m/z 43, 71, 89 and 249 for a crater, in which there was a visible contaminant at the centre. The CN^- image confirms that the contaminant is on the outmost surface of the clearcoat (represented by CN^-). The contaminant has more abundant negative ions at m/z 43, 71, 89 and 249, as well as positive ions of $C_2H_5^+$, $C_3H_5^+$ and $C_4H_9^+$ (positive ions not shown). As shown in Fig. 9b, when a suspect additive (chemical composition not known to us) was analysed, the additive contained the same mass fragments that were evident in the contaminant.

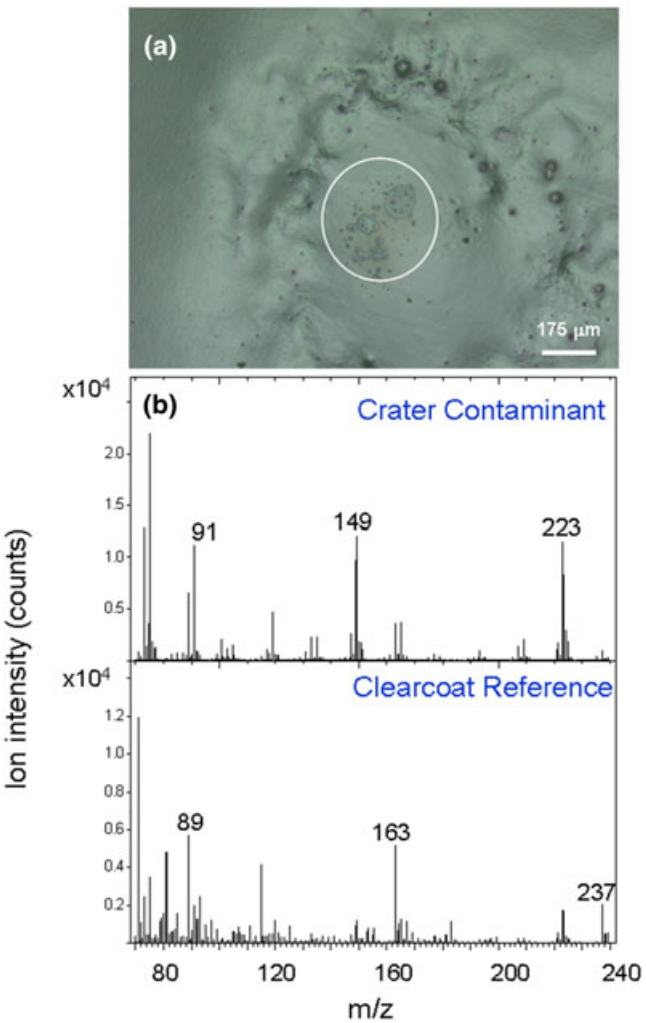

Figure 8. (a) Optical image and (b) negative secondary ion mass spectra collected from a crater (upper panel) and a clearcoat reference (lower panel).

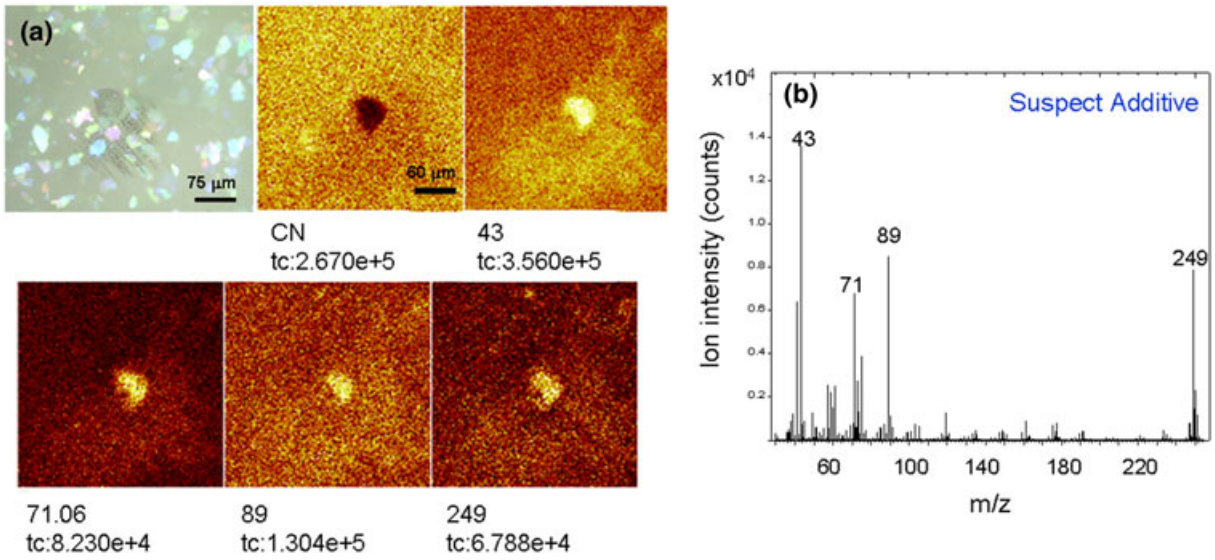

Figure 9. (a) Optical image and negative secondary ion images collected from a crater and (b) negative secondary ion mass spectrum collected from the suspect additive.

From the ToF-SIMS results shown in Fig. 9, we infer that the crater formed because of aggregation of the suspect additive either before or during application to the surface.

Fatty acid contaminant

Another common contaminant detected in craters by ToF-SIMS is fatty acids. Fatty acids or their derivatives have many uses, and when detected in a crater, although not restricted to, it can sometimes indicate that the crater has been caused by a personal care product.

Presented in Fig. 10 is an example showing the detection of long chain fatty acids palmitate $C_{16}H_{31}O_2^-$ (255) and stearate $C_{18}H_{35}O_2^-$ (283) in a crater that were not detected in the reference clearcoat. They were in a circular shape and spanned approximately half a millimetre. These two fatty acids are the most common ones encountered. They are readily identifiable because we have not seen any other ions with decent abundance around the m/z positions

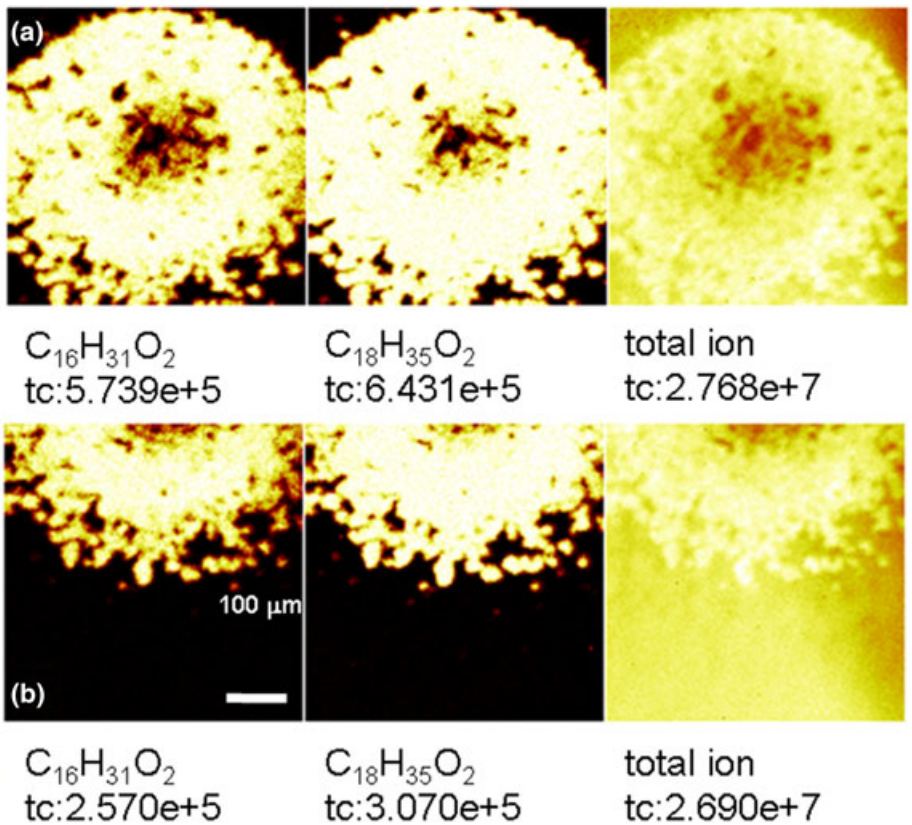

Figure 10. Ion images of $C_{16}H_{31}O_2^-$ (palmitate), $C_{18}H_{35}O_2^-$ (stearate)$^-$ and the total ion collected from (a) a crater and (b) its edge.

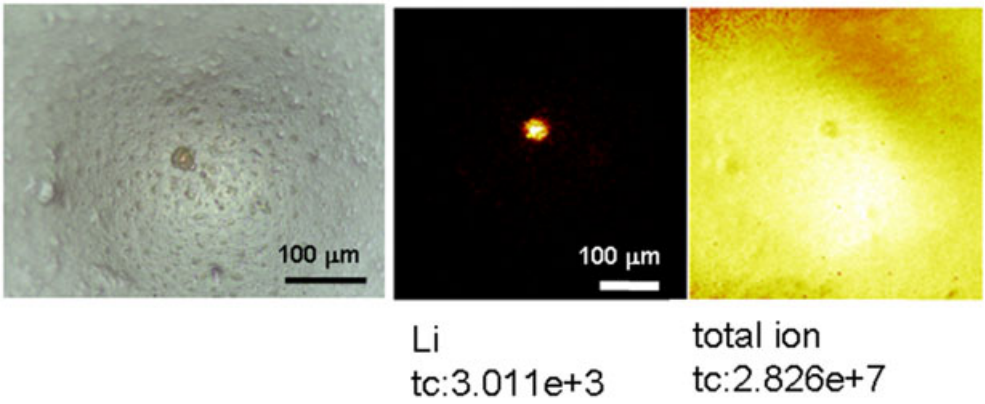

Figure 11. Optical image and Li^+ and the total ion images collected from a crater. The Li^+ corresponds with the small circular contaminant visible in the optical image.

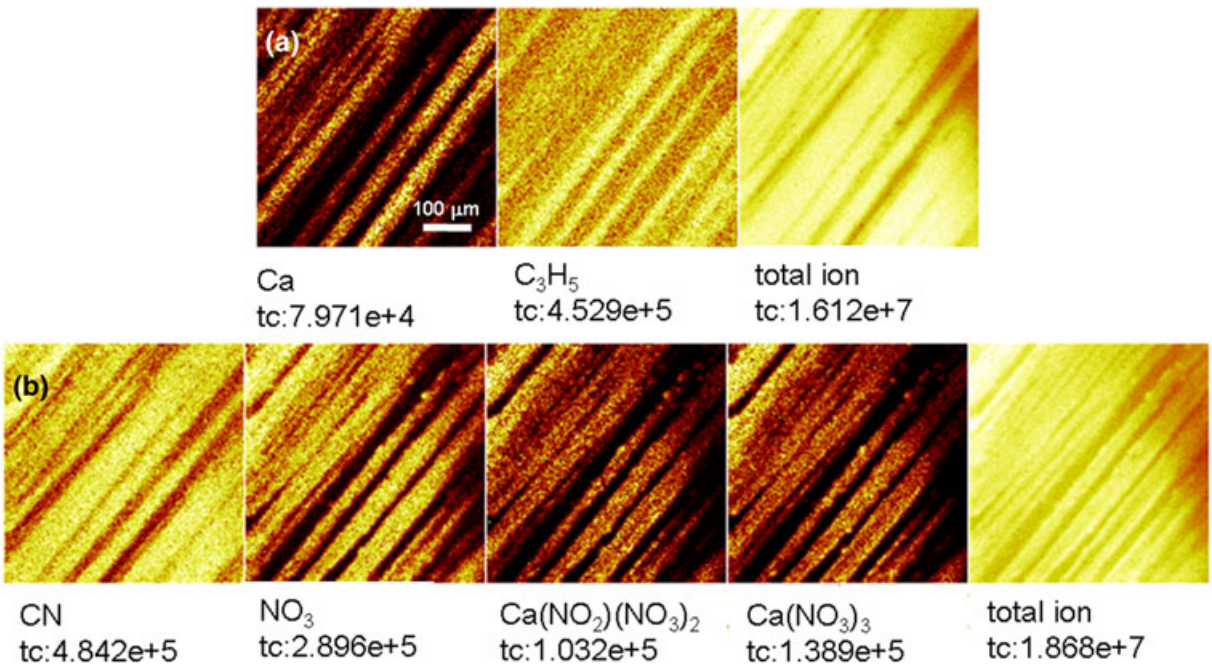

Figure 12. (a) Positive and (b) negative secondary ion images collected from a crater showing streaks running through it.

of the two fatty acids. With their relatively long hydrocarbon chains, the fatty acids are characterized as having low surface energy. Therefore, concentration/aggregation of fatty acids on the surface to be painted or in the paint provides an environment prone to paint cratering.

From our experience, shorter chain fatty acids, such as caprylic acid ($C_8H_{16}O_2$) and capric acid ($C_{10}H_{20}O_2$), also cause craters. Their deprotonated molecular ions are $C_8H_{15}O_2^-$ (143) and $C_{10}H_{19}O_2^-$ (171), respectively. Sometimes also detected is a positive ion at m/z 551.5, which is assigned to $C_{35}H_{67}O_4^+$, most likely from glyceryl dipalmitate ($C_{35}H_{68}O_5$), a fat, with the removal of the OH group of the molecule. Fats, which are similar to fatty acids in terms of having a low surface energy, also tend to cause craters.

Additional examples

Other species can also lead to crater formation. The ToF-SIMS analysis of a paint crater detected a high level of hydrocarbon throughout the crater, and as shown in Fig. 11, lithium was detected near the centre. Considering the crater came from an automotive plant where lubricants are used and the fact that there is even a slight increase in hydrocarbon on the spot (not shown), we infer that the cause of the crater may be a lithium-based grease, even though no specific ions pointing to the chemical structure of the grease were identified.

Finally, we present a case where the formation of a crater is difficult to explain using the surface energy model. Figure 12 shows an example where streaks of calcium nitrate were observed. In this figure, Ca^+, a typical hydrocarbon ion $C_3H_5^+$, CN^- (arising from the clearcoat), NO_3^-, $Ca(NO_2)(NO_3)_2^-$ and $Ca(NO_3)_3^-$ are shown. Based on the detection of calcium nitrate, which is commonly used in concrete, we were able to determine that the crater was caused when concrete work was being performed near the paint line. However, because the detection of calcium nitrate does not fit the surface energy model, it is postulated that the crater may have formed by the incompatibility of the paint with the inorganic

calcium nitrate. This explanation may be somewhat speculative, but nevertheless, the detection of the contaminant still provides valuable information.

Another scenario is that the crater might be caused by a volatile, low surface energy contaminant, which would have evaporated during the baking process. In this scenario, we obviously assumed that the volatile contaminant was associated with the calcium nitrate.

There are also instances when the ToF-SIMS analysis of the surface of the crater does not detect any differences from the rest of the painted surface. In these cases, either whatever caused the crater is no longer present on the surface or the crater originated below the surface being analysed. It is worth mentioning that in these cases, the craters tend to be rather shallow and large.

Conclusions

The surface sensitivity, selectivity in identifying chemical structures and superior mapping capabilities make ToF-SIMS a valuable technique in attempting to determine the causes of paint craters. Unfortunately, ToF-SIMS is not quantitative without the use of standards, and identification of an uncommon contaminant can be difficult because the reference spectra in commercial spectral libraries are limited. However, as shown in this article, ToF-SIMS is invaluable in detecting common cratering agents such as siloxanes, fluorocarbons and fatty acids, as well as many others. We also demonstrated that if a suspect material is provided, ToF-SIMS can match the contaminant to it.

References

[1] N. K. Akafuah, S. Poozesh, A. Salaimeh, G. Patrick, K. Lawler, K. Saito, *Coatings*, **2016**, *6*, 24.
[2] L. O. Kornum, H. K. R. Nielsen, *Prog. Org. Coat.*, **1980**, *8*, 275–324.
[3] C. K. Schoff, *J. Coatings Technol.*, **1999**, *71*(888), 57–73.
[4] W. D. Harkins, A. Feldman, Films, *J. Am. Chem. Soc.*, **1922**, *44*, 2665–2685.
[5] P. G. de Gennes, *Rev. Mod. Phys.*, **1985**, *57*, 827–863.
[6] D. E. Packham, *Int. J. Adhesion Adhesives*, **1996**, *16*, 121–128.
[7] M. K. Chaudhury, *Mater. Sci. Eng. R*, **1996**, *16*, 97–159.
[8] D. Bonn, J. Eggers, J. Indekeu, J. Meunier, E. Rolley, *Rev. Mod. Phys.*, **2009**, *81*, 739–805.
[9] S. Seraj, Z. Ranjbar, A. Jannesari, *Prog. Org. Coat.*, **2014**, *77*, 1735–1740.
[10] K. Grundke, S. Michel, G. Knispel, A. Grundler, *Colloids Surf. A: Physicochem. Eng. Aspects*, **2008**, *317*, 598–609.
[11] V. V. Verkholandtsev, *Eur. Coatings J.*, **2003**, *9*, 18–26.
[12] http://multimedia.3m.com/mws/media/624307O/3m-fluorosurfactants-for-paints-and-coating.pdf (as of August 9, 2017).
[13] P. L. Evans, L. W. Schwartz, R. V. Roy, *J. Colloid Interface Sci.*, **2000**, *227*, 191–205.
[14] A. Benninghoven, *Angew. Chem. Int. Ed. Engl.*, **1994**, *33*, 1023–1043.
[15] J. C. Vickerman, N. Winograd, *Int. J. Mass Spectrum.*, **2015**, *377*, 568–579.
[16] http://www.tasconusa.com/media/usa_neu/downloads/TAS-AN-03E.pdf (as of August 9, 2017).
[17] http://www.surfacesciencewestern.com/industrial-solutions/automotive/tof-sims-analysis-of-crater-defect/ (as of August 9, 2017).
[18] U. Wolff, H. Thomas, M. Osterhold, *Prog. Org. Coat.*, **2004**, *51*, 163–171.
[19] M. Inoue, A. Murase, M. Sugiura, *Anal. Sci.*, **2004**, *20*, 1623–1628.
[20] S. J. Hinder, J. F. Watts, G. C. Simmons, C. Lowe, *Surf. Interface Anal.*, **2008**, *40*, 436–440.
[21] M. Brenda, R. Döring, U. Schernau, *Prog. Org. Coat.*, **1999**, *35*, 183–189.
[22] H.-Y. Nie, *Anal. Methods*, **2013**, *5*, 4911–4920.
[23] M. L. Manier, D. S. Cornett, D. L. Hachey, R. M. Caprioli, *J. Am. Soc. Mass Spectrum.*, **2008**, *19*, 666–670.
[24] R. N. S. Sodhi, *Analyst*, **2004**, *129*, 483–487.
[25] C. Bao, K.-Q. Xu, C.-Y. Tang, W. M. Lau, C.-B. Yin, Y. Zhu, J. Mei, J. Lee, D. Hui, H.-Y. Nie, Y. Liu, *ACS Adv. Mater. Interface*, **2015**, *7*, 8515–8524.